AAS 19-484

SURFING IN THE PHASE SPACE OF EARTHS OBLATENESS AND THIRD BODY PERTURBATIONS

Camilla Colombo[*], Francesca Scala[†], and Ioannis Gkolias[‡]

In this work, we exploit the luni-solar perturbations for the post-mission disposal of satellites in high-altitude orbits. Starting from the double-averaged dynamical system, the representation of the dynamics is reduced to a one degree-of-freedom Hamiltonian, depending on the the orbit eccentricity and the perigee orientation in the equatorial frame. An analytical method is proposed for designing the disposal maneuver with the goal to achieve natural re-entry by exploiting the long-term effect of the natural perturbations, enhanced by impulsive maneuvers. The optimal initial conditions to apply the impulsive maneuver, such that a fast re-entry is achieved, are selected via a gradient based method in the phase space.

INTRODUCTION

The implementation of end-of-life disposal strategies is mandatory for Earth's satellite in low Earth orbit (LEO) and geostationary orbits (GEO). Nevertheless for other cases, like Highly Elliptical Orbits (HEOs), the disposal is recommended by the Inter-Agency Space Debris Coordination Committee. In this work, the post-mission disposal of HEOs satellite about the Earth is designed by exploiting the luni-solar perturbations. The dynamics of this region is mainly influenced by the effects of the third body perturbations due to the gravitational attraction of the Moon and the Sun, coupled with the Earth's oblateness. The orbit evolution can be described through the variation of the Keplerian elements double-averaged over the orbital periods of the spacecraft and the perturbing bodies around the main planet (Earth). A representation of the system with respect to the plane of the perturbing body yields a one degree of freedom Hamiltonian system.[1]

Some past works proposed the design of a spacecraft maneuver in the phase space. For example, an efficient series of maneuvers to shape the orbits and phasing of the two orbiters of the GRAIL mission to the Moon was devised using a geometric method based on the change of the eccentricity vector.[2] Moreover, the phase space of eccentricity and anomaly of perigee was employed in the design of the end-of-life disposal orbit for the INTEGRAL mission.[3] Taking a different approach than previous works, where the optimal maneuver was found through the propagation of the double-averaged dynamical model, in this paper, an analytical model is proposed for designing the disposal maneuver, with no numerical propagation involved. This method aims to achieve a natural re-entry by exploiting the long-term effect of the orbital perturbations, enhanced also by impulsive

[*]Ph.D., Associate Professor, Department of Aerospace Science and Technology, Politecnico di Milano, Via La Masa 34, 20156, Milano, Italy. email: camilla.colombo@polimi.it

[†]M.Sc. Space Engineering graduate, Department of Aerospace Science and Technology, Politecnico di Milano, Via La Masa 34, 20156, Milano, Italy. email: francesca.scala@mail.polimi.it

[‡]Ph.D., Research Fellow, Department of Aerospace Science and Technology, Politecnico di Milano, Via La Masa 34, 20156, Milano, Italy. email: ioannis.gkolias@polimi.it

maneuvers. The optimal initial conditions during the natural evolution of the argument of perigee and the orbit eccentricity are selected such that, through an impulsive maneuver, the new orbit conditions will lead to a natural increase of the orbit eccentricity until re-entry is reached. The design of the disposal maneuver is fully done on the reduced phase space. A contour line of the Hamiltonian, identified by the spacecraft initial condition, represents the long-term evolution of the satellite under the natural dynamics.

In this work, instead of considering the model formulation with respect to the Moon plane, as in several works,[3,4] an equivalent representation was used: we assume a reference frame which has the central planet's equator as the fundamental plane. Moreover, the effect of J_2 zonal harmonics is introduced in the model. After the recovery of the reduced one-degrees-of-freedom Hamiltonian, the analytical representation is used to design the maneuver strategy in two different systems: the Venus-Sun system and the Earth-Moon-Sun system. The analysis aims to study first the feasibility of the fully-analytical method for maneuver design in a simple system, involving only one external perturbing body: an orbiter around Venus feels the effect of the Sun gravitational attraction. Once the model is validated for this system, it is applied to the Earth's satellite case. In particular, the INTEGRAL disposal is considered, starting from the analysis already done in literature.[4,5] In this case, the fully-analytical method for maneuver design is affected by the problem of the elimination of the node, producing discordant results with respect to the numerical propagation in time.

The work is organized as follows: first, the model formulation is presented, where the double-averaged formulation is validated against the full model. Then, the reduced Hamiltonian formulation is computed, to produce two-dimensional phase space maps for maneuver design. Finally, the disposal strategy is briefly presented, and the reduced Hamiltonian model is applied to two scenarios: a Venus' orbiter and the INTEGRAL mission.

MODEL FORMULATION

The generic representation for the dynamics of a satellite around a generic planet under the influence of the third body perturbation is now derived.

Orbital Perturbations

By using the perturbed Keplerian motion for a massless spacecraft, the orbit evolution in time can be represented through the Hamiltonian formulation as:

$$\mathcal{H} = \mathcal{H}_{kep} - \mathcal{R} = -\frac{\mu}{2\,a} - \mathcal{R}_{zonal} - \mathcal{R}_{3b}, \tag{1}$$

where the first term represents the Keplerian contribution, with μ the planet's gravitational parameter and a the satellite's semi-major axis, and the second term $\mathcal{R}$ is the disturbing function due to the effects of natural orbit perturbations. In this work only zonal harmonics and third body effects are considered. The analytical expression of the zonal effect, due to the gravitational field of the planet, is written in terms of Legendre polynomials as:[6]

$$\mathcal{R}_{zonal} = -\frac{\mu}{r}\sum_{l=2}^{\infty} J_l \left(\frac{R_\alpha}{r}\right)^l P_l(\sin\delta), \tag{2}$$

where J_l are the zonal harmonic coefficients, R_α is the planet mean equatorial radius, r is the satellite position vector, $P_l(\sin\delta)$ are the the zeroth order associated Legendre polynomials of degree l

and δ is the geocentric latitude. The satellite's position vector can be expressed in the equatorial frame in terms of its orbital elements:[6]

$$\begin{pmatrix} x \\ y \\ z \end{pmatrix} = R_3(\Omega)R_1(i)R_3(\omega + f) \begin{pmatrix} r \\ 0 \\ 0 \end{pmatrix}, \tag{3}$$

where Ω is the right ascension of the ascending node (RAAN), i is the orbit inclination, ω is the argument of perigee, and f is the true anomaly of the satellite, all measured in the equatorial frame. The expressions for the matrixes R_1 and R_3 are here reported in function of a generic angle θ:

$$R_3(\theta) = \begin{pmatrix} \cos\theta & -\sin\theta & 0 \\ \sin\theta & \cos\theta & 0 \\ 0 & 0 & 1 \end{pmatrix}, \tag{4}$$

$$R_1(\theta) = \begin{pmatrix} 1 & 0 & 0 \\ 0 & \cos\theta & -\sin\theta \\ 0 & \sin\theta & \cos\theta \end{pmatrix}. \tag{5}$$

The position along the orbit is written in terms of the true anomaly, while the latitude is a function of inclination, argument of perigee and true anomaly:

$$r = \frac{a(1-e^2)}{1+\cos f}, \tag{6}$$

$$\sin\delta = \frac{z}{r} = \sin(\omega + f)\sin i, \tag{7}$$

where e is the eccentricity, ω the satellite argument of perigee, f is the satellite true anomaly, and i is the inclination of the orbit. Finally, the third body contribution is modelled using the Legendre polynomials in terms of the parallactic ratio $\delta = a/r_{3b}$:[7,8]

$$\mathcal{R} = \frac{\mu_{3b}}{r_{3b}} \sum_{l=2}^{\infty} \delta^l \left(\frac{r}{a}\right)^l P_l[\cos S], \tag{8}$$

where μ_{3b} is the third body's gravitational parameter, r_{3b} is the third body's position vector with respect to the central planet, r is the satellite position vector, a is the satellite semi-major axis, and S is the angle between the satellite and the third body position vector measured from the central planet. This angle is expressed through the scalar product of the two vector $\mathbf{r}$ and $\mathbf{r}_{3b}$:[7]

$$\cos S = \frac{\mathbf{r}\cdot\mathbf{r}_{3b}}{r\, r_{3b}} = \hat{\mathbf{r}}\cdot\hat{\mathbf{r}}_{3b}. \tag{9}$$

The $\cos S$ term is defined as function of satellite's and a perturbing body's position vector. To continue the derivation, it is necessary to express it in terms of satellite's orbital elements. The spacecraft position vector is therefore expressed in the perifocal frame. Since only the unit vector enters in the $\cos S$ relation, the expression is recovered by dividing the position vector by its magnitude as:

$$\hat{\mathbf{r}} = \hat{\mathbf{P}}\cos f + \hat{\mathbf{Q}}\sin f, \tag{10}$$

where $\hat{\mathbf{P}}$ and $\hat{\mathbf{Q}}$ are respectively the unit vector in direction of the eccentricity vector and the one in the semilatus rectum direction on the orbital plane.

They can be expressed through a series of rotations:[7,8]

$$\hat{\mathbf{P}} = R_3(\Omega)R_1(i)R_3(\omega)\hat{I} \qquad \hat{\mathbf{Q}} = R_3(\Omega)R_1(i)R_3\left(\omega + \frac{\pi}{2}\right)\hat{I} - \tag{11}$$

Starting from the Eq. (10) and considering the unit vector in the direction of the third body as $\hat{\mathbf{r}}_{\mathbf{3b}}$, the $\cos S$ term can be written as an explicit relation of the true anomaly of the satellite:

$$\cos S = A_{3b}\cos f + B_{3b}\sin f, \tag{12}$$

where $A_{3b} = \hat{\mathbf{P}} \cdot \hat{\mathbf{r}}_{\mathbf{3b}}$ and $B_{3b} = \hat{\mathbf{Q}} \cdot \hat{\mathbf{r}}_{\mathbf{r3b}}$, and they are independent from the true anomaly f. This formulation reduces the generic expression of the third body potential to a function of A_{3b}, B_{3b}, f and r only:[5]

$$\mathcal{R} = \frac{\mu_{3b}}{r_{3b}} \sum_{l=2}^{\infty} \delta^l F_l(A_{3b}, B_{3b}, r, f). \tag{13}$$

At this point in order to develop the analytical theory, the position vector of the third body must be expressed in the planet centered inertial frame, with the equator as the reference plane.[6] In case of the Sun, its position is simply given by:

$$\begin{pmatrix} x_\odot \\ y_\odot \\ z_\odot \end{pmatrix} = R_1(\epsilon)R_3(\lambda_{ecl}) \begin{pmatrix} r_\odot \\ 0 \\ 0 \end{pmatrix}, \tag{14}$$

where $r_\odot$ is the magnitude of the Sun position vector, λ_{ecl} is the ecliptic longitude of the Sun, and ϵ is the planet's obliquity on the ecliptic. In this work, $r_\odot$ and ϵ are considered constant in time in the first approximation (i.e. the planet is considered on a circular orbit around the Sun). Similarly, in case the third body is a natural satellite (Moon) of the planet, its position is given by:

$$\begin{pmatrix} x_{\leftmoon} \\ y_{\leftmoon} \\ z_{\leftmoon} \end{pmatrix} = R_3(\Omega_{\leftmoon})R_1(i_{\leftmoon})R_3(\omega_{\leftmoon} + f_{\leftmoon}) \begin{pmatrix} r_{\leftmoon} \\ 0 \\ 0 \end{pmatrix}, \tag{15}$$

where $\Omega_{\leftmoon}$ is the right ascension of the ascending node (RAAN) of the Moon, $i_{\leftmoon}$ is the Moon orbital inclination, $\omega_{\leftmoon}$ is the Moon argument of perigee, and $f_{\leftmoon}$ is the true anomaly of the Moon, all measured in the equatorial frame. In this case $r_{\leftmoon}$ varies in time, since the orbit of the Moon is considered elliptical:

$$r_{\leftmoon} = \frac{a(1 - e_{\leftmoon}^2)}{1 + e_{\leftmoon}\cos f_{\leftmoon}}. \tag{16}$$

In order to develop a first preliminary model for the satellite secular time evolution, only the J_2 zonal harmonic contribution due to the planet's oblateness is considered and the third body perturbation is expanded up to the fourth order to have a proper representation for Highly Elliptical Orbits.[3] Under these assumptions, the disturbing potentials due to J_2 and the third body attraction become:

$$\mathcal{R}_{zonal,J2} = -\frac{\mu J_2}{2\,r}\left(\frac{R_\alpha}{r}\right)^2 (3\sin\delta^2 - 1), \tag{17}$$

$$\mathcal{R}_{3b} = \frac{\mu_{3b}}{r_{3b}} \sum_{l=2}^{4} \delta^l F_l(A_{3b}, B_{3b}, r, f), \tag{18}$$

where the second, third and fourth order terms from the polynomial expansion in $\mathcal{R}_{3b}$ are functions of $\cos S$, which depends of A_{3b} and B_{3b} as in Eq. (12):

$$F_2 = \left(\frac{r}{a}\right)^2 P_2[\cos S] = \frac{1}{2}\left(\frac{r}{a}\right)^2 \left(3\cos^2 S - 1\right), \tag{19}$$

$$F_3 = \left(\frac{r}{a}\right)^3 P_3[\cos S] = \frac{1}{2}\left(\frac{r}{a}\right)^3 \left(5\cos^3 S - 3\cos S\right), \tag{20}$$

$$F_4 = \left(\frac{r}{a}\right)^4 P_4[\cos S] = \frac{1}{8}\left(\frac{r}{a}\right)^4 \left(35\cos^4 S - 30\cos^2 S + 3\right). \tag{21}$$

Averaging Procedure

Since this work focuses on the study of the long-term dynamics of the satellites, the first step is to cancel out the short-term effects due to the true anomaly variation along the orbit. This procedure acts as a low pass filter to cancel out the high-frequency variations. The approach consists of a double averaging of the disturbing function. The first averaging is done over the satellite's orbital period, and to do so, the disturbing function is written in terms of the eccentric anomaly and the other orbital elements of the space vehicle:[8]

$$\bar{\mathcal{R}} = \frac{1}{2\pi}\int_0^{2\pi} \mathcal{R} dM = \frac{1}{2\pi}\int_0^{2\pi} \mathcal{R}\left(1 - e\cos E\right) dE. \tag{22}$$

The second averaging, which involves only the third body disturbing function, is done over the third body orbital period. In this case the averaging is done re-conducing the terms to the true anomaly, in order not to have $\cos$ or $\sin$ terms in the denominator, yielding to an easier computation:

$$\bar{\bar{\mathcal{R}}} = \frac{1}{2\pi}\int_0^{2\pi} \bar{\mathcal{R}} dM_{3b} = \frac{1}{2\pi}\int_0^{2\pi} \bar{\mathcal{R}} \frac{(1-e_{3b})^{3/2}}{(e_{3b}\cos f_{3b} + 1)^2} df_{3b}. \tag{23}$$

The analytical expression of the double-averaged of the potential is cross-checked with literature results.[8]

Single-averaged disturbing function The complete procedure for the single-averaging is now reported, where all the computation were derived analytically with Mathematica® software. At first, the potentials shall be written in terms of orbital elements, then by making explicit the dependence on the true anomaly, the integration is performed.

Zonal disturbing function. The position along the orbit is written in terms of the true anomaly, while the latitude is a function of inclination, argument of perigee and true anomaly, as reported in Eq. (6) and (7). This procedure yields a new expression of the zonal disturbing potential:

$$\mathcal{R}_{J2} = -\frac{\mu\, J_2\, R_\alpha^2}{4} \frac{2 - 3\sin^2 i + 3\sin^2 i(\cos 2\omega \cos 2f - \sin 2\omega \sin 2f)}{\left((a(1-e^2))/(1+\cos f)\right)^3}. \tag{24}$$

Since the averaging is done over the mean anomaly M, an efficient way to perform the integral is to write the radius and the mean anomaly $(r,\ M)$ in terms of the true anomaly f:[9]

$$dM = \frac{r^2}{a^2(1-e^2)^{1/2}} df = \frac{(1-e)^{3/2}}{(e\cos f + 1)^2} df, \tag{25}$$

$$r = \frac{a(1-e^2)}{1 + e\cos f}, \tag{26}$$

and the results of the integration for the zonal harmonics terms is:

$$\bar{\mathcal{R}}_{J_2} = \frac{1}{2\pi}\int_0^{2\pi} \mathcal{R}_{J_2} dM = \frac{\mu J_2 R_\alpha^2}{8\, a^3 (1-e^2)^{3/2}}(1+3\cos 2i). \tag{27}$$

Therefore, the disturbing potential due to J_2 depends only on three orbital parameters: the semi-major axis a, the eccentricity e, and the orbit inclination i. Hence, after evaluating the derivative of the disturbing potential respect to the orbital elements, the time variation due to J_2 can be recovered.

Third body disturbing function. The derivation in this section is valid for both the Sun and the Moon effect.[8] The procedure consists in canceling out the contribution due to the variation of the true anomaly along the orbit. Therefore, it is better to express the Eq. (18) in terms of the orbital elements. For either the Sun and the Moon, the general expression of the potential can be expressed as follows, without loss of generality:

$$\mathcal{R}_{3b} = \frac{\mu_{3b}}{r_{3b}} \sum_{l=2}^{4} \delta_{3b}^l \, F_l(A_{3b}, B_{3b}, r, f). \tag{28}$$

The terms to be averaged are r and f, since they are the only terms in Eq. (28) that vary over the orbital period. The integral is computed analytically, by solving different order terms one per time. For each F_i $(i = 2:4)$ function the results from the computations are reported. The second order term is obtained considering the coefficient $l = 2$ in the Eq. (28):

$$\mathcal{R}_{3b,2} = \frac{\mu_{3b}}{r_{3b}} \delta_{3b}^2 \, F_2(A_{3b}, B_{3b}, r, f). \tag{29}$$

The potential is now expressed using the trigonometric relations of sine and cosine and introducing the expression of $\cos S$:

$$\begin{aligned} \mathcal{R}_{3b,2} =& \frac{\mu_{3b}}{r_{3b}} \left(\frac{1}{2}\delta_{3b}^2 \left(\frac{r}{a}\right)^2 \left(3\cos^2 S - 1\right)\right), \qquad \text{with} \qquad \cos S = A_{3b}\cos f + B_{3b}\sin f \\ =& \frac{1}{4}\frac{\mu_{3b}}{r_{3b}} \delta^2 \left(\frac{r}{a}\right)^2 \left(3\left(A_{3b}^2 - B_{3b}^2\right)\cos 2f + 6A_{3b}B_{3b}\sin 2f + 3(A_{3b}^2 + B_{3b}^2) - 2\right). \end{aligned} \tag{30}$$

Performing the integration, the first average disturbing function for the second order becomes:[7,8]

$$\bar{\mathcal{R}}_{3b,2} = \frac{\mu_{3b}}{4r_{3b}} \delta^2 \left(3A_{3b}^2\left(4e^2+1\right) - 3B_{3b}^2\left(e^2-1\right) - 3e^2 - 2\right). \tag{31}$$

The same procedure is followed for the third and the fourth order terms:[7,8]

$$\bar{\mathcal{R}}_{3b,3} = \frac{5\mu_{3b}}{16 r_{3b}} \delta^3 A_{3b} e \left(-5A_{3b}^2\left(4e^2+3\right) + 15B_{3b}^2\left(e^2-1\right) + 9e^2 + 12\right), \tag{32}$$

$$\begin{aligned} \bar{\mathcal{R}}_{3b,4} =& \frac{3\mu_{3b}}{64 r_{3b}} \delta^4 \Big(35A_{3b}^4\left(8e^4+12e^2+1\right) - 10A_{3b}^2\big(7B_{3b}^2\left(6e^4-5e^2-1\right) + 18e^4 + \\ &+ 41e^2 + 4\big) + 35B_{3b}^4\left(e^2-1\right)^2 + 10B_{3b}^2\left(3e^4+e^2-4\right) + 15e^4 + 40e^2 + 8\Big). \end{aligned} \tag{33}$$

This results in a final single-averaged Hamiltonian expression for the time evolution of the satellite's orbit:

$$\begin{aligned}\bar{\mathcal{H}} =& -\frac{\mu}{2\,a} - \bar{\mathcal{R}}_{zonal} - \bar{\mathcal{R}}_{3b} \\ =& -\frac{\mu}{2\,a} - \frac{\mu J_2 R_\alpha^2}{8\,a^3(1-e^2)^{3/2}}(1+3\cos 2i) \\ & -\frac{\mu_{3b}}{4r_{3b}}\delta^2\left(3A_{3b}^2\left(4e^2+1\right)-3B_{3b}^2\left(e^2-1\right)-3e^2-2\right)+ \\ & -\frac{5\mu_{3b}}{16r_{3b}}\delta^3 A_{3b} e\left(-5A_{3b}^2\left(4e^2+3\right)+15B_{3b}^2\left(e^2-1\right)+9e^2+12\right)+ \\ & -\frac{3\mu_{3b}}{64r_{3b}}\delta^4\Big(35A_{3b}^4\left(8e^4+12e^2+1\right)-10A_{3b}^2\Big(7B_{3b}^2\left(6e^4-5e^2-1\right)+18e^4+ \\ & +41e^2+4\Big)+35B_{3b}^4\left(e^2-1\right)^2+10B_{3b}^2\left(3e^4+e^2-4\right)+15e^4+40e^2+8\Big).\end{aligned} \tag{34}$$

Double-averaged disturbing function. The double-averaging technique consists now in averaging the single-averaged expression over the orbital period of the perturbing body. During the averaging process over the perturbing body's mean anomaly, the rest of orbital elements are considered constant. The parameters that vary during the procedure are r_{3b} and both A_{3b} and B_{3b} terms. The analytical expression of these two terms is dependent on the third body considered. On the other hand, the term related to the J_2 zonal harmonic disturbance does not depend on the third body, so it is not necessary to average it another time. The results of the double-averaging procedure are now reported in case of both the Sun and a natural satellite, like the Moon, disturbances.

Sun double-averaged disturbing function. The Sun perturbation depends on its distance and position vector with respect to the central body. The latter is expressed in the equatorial frame thanks to the ecliptic longitude of the Sun λ_{ecl} and the planet's obliquity on the ecliptic ϵ. In this case, the $\cos S$ term can be expressed as

$$\cos S = \left(\hat{P}\cdot\hat{\mathbf{r}}_\odot\right)\cos f + \left(\hat{Q}\cdot\hat{\mathbf{r}}_\odot\right)\sin f = A_\odot\cos f + B_\odot \sin f, \tag{35}$$

where the coefficients $A_\odot$ and $B_\odot$ are:[8]

$$\begin{aligned}A_\odot =& \cos\lambda_{ecl}(\cos\omega\cos\Omega - \sin\omega\sin\Omega\cos i)+ \\ & \sin\lambda_{ecl}(\cos\epsilon\cos\omega\sin\Omega+\cos\epsilon\cos\Omega\sin\omega\cos i+\sin\epsilon\sin\omega\sin i),\end{aligned} \tag{36}$$

$$\begin{aligned}B_\odot =& \cos\lambda_{ecl}(-\cos\Omega\sin\omega - \cos\omega\sin\Omega\cos i)+ \\ & \sin\lambda_{ecl}(\cos\epsilon\sin\omega\sin\Omega+\cos\epsilon\cos\omega\cos\Omega\cos i+\sin\epsilon\cos\omega\sin i).\end{aligned} \tag{37}$$

For most of Solar system planets, the eccentricity of the orbit around the Sun can be approximated to the circular case as a fist preliminary approximation. In addition, since the ecliptic longitude of the Sun varies in one year, during the motion of the Earth along its orbit, from 0° to 360°, as a first approximation, the double averaging is done over the ecliptic longitude instead of the mean anomaly. By using these approximations, the double-averaged disturbing function is computed with the following integration:

$$\frac{1}{2\pi}\int_0^{2\pi}\bar{\mathcal{R}}_\odot\, d\lambda_{ecl}. \tag{38}$$

The final expression is the following:[8]

$$\begin{aligned}\bar{\bar{\mathcal{R}}}_{\odot,2} =& \frac{\mu_\odot\, a^2}{16\, r_\odot^3}\Big[-8 - 12\, e^2 + 3(2 + 3\, e^2 + 5\, e^2 \cos 2\omega)\cos^2\Omega + \\ & - 15\, e^2 \sin 2\omega \sin 2\Omega \cos i - 3(-2 - 3\, e^2 + 5\, e^2 \cos 2\omega)\sin^2\Omega \cos^2 i + \\ & - \Big(-3(\cos\epsilon \sin\omega \sin\Omega + \cos\epsilon \cos\omega \cos\Omega \cos i + \cos\omega \sin\epsilon \sin i)^2 + \\ & + 3\, e^2(-\cos\epsilon \sin\omega \sin\Omega + \cos\epsilon \cos\omega \cos\Omega \cos i + \cos\epsilon \cos\omega \sin i) \\ & - 3(\cos\epsilon \cos\omega \sin\Omega + \cos\epsilon \cos\Omega \sin\omega \cos i + \sin\epsilon \sin\omega \sin i)^2 + \\ & - 12\, e^2(\cos\epsilon \cos\omega \sin\Omega + \cos\epsilon \cos\Omega \sin\omega \cos i + \sin\epsilon \sin\omega \sin i)^2\Big)\Big].\end{aligned} \tag{39}$$

Since the circular case is adopted, as demonstrated for the Lunar case,[8] the third-order term is null (in particular all the odd order terms would be zero).

$$\bar{\bar{\mathcal{R}}}_{\odot,3} = 0. \tag{40}$$

The expression for $\bar{\bar{\mathcal{R}}}_{\odot,4}$ term is lengthy and therefore not reported here for concision. In conclusion the overall expression is function of:

$$\bar{\bar{\mathcal{R}}}_{\odot} = \bar{\bar{\mathcal{R}}}_{\odot}(a,\, e,\, i,\, \omega,\, \Omega,\, -;\, \epsilon,\, r_\odot,\, \mu_\odot), \tag{41}$$

where the satellite semi-major axis a is a constant of motion.

Moon double-averaged disturbing function. In the case a natural satellite, like the Moon for the Earth system, is considered as the third body, no assumptions are done and the perturbing body orbit is considered elliptical and inclined, and differently from most previous works, the derivation was done in the equatorial frame and not in the Moon plane.[3,4,8,10,11] The mean anomaly is a linear function of time: $M = n(t - t_0)$. As for the case of the single averaging over the satellite f, the Moon true anomaly is averaged out through the mean anomaly of the third body $M_{\leftmoon}$. In particular $A_{\leftmoon}$ and $B_{\leftmoon}$ have the following expression:

$$\begin{aligned}A_{\leftmoon} =& \sin\omega((\cos i \cos i_{\leftmoon} \cos(\Omega - \Omega_{\leftmoon}) + \sin i \sin i_{\leftmoon})\sin(\omega_{\leftmoon} + f_{\leftmoon}) + \\ & - \cos i \cos(\omega_{\leftmoon} + f_{\leftmoon})\sin(\Omega - \Omega_{\leftmoon})) + \cos\omega(\cos(\omega_{\leftmoon} + f_{\leftmoon}) \\ & \cos(\Omega - \Omega_{\leftmoon}) + \cos i_{\leftmoon} \sin(\omega_{\leftmoon} + f_{\leftmoon} \sin(\Omega - \Omega_{\leftmoon})),\end{aligned} \tag{42}$$

$$\begin{aligned}B_{\leftmoon} =& \cos\omega \sin i \sin i_{\leftmoon} \sin(\omega_{\leftmoon} + f_{\leftmoon}) + (\cos i \cos\omega \cos\Omega - \sin\omega \sin\Omega) \\ & (\cos i_{\leftmoon} \cos\Omega_{\leftmoon} \sin(\omega_{\leftmoon} + f_{\leftmoon}) + \cos(\omega_{\leftmoon} + f_{\leftmoon} \sin\Omega_{\leftmoon})) + \\ & + (\cos\Omega \sin\omega + \cos i \cos\omega \sin\Omega)(-\cos(\omega_{\leftmoon} + f_{\leftmoon}) \cos\Omega_{\leftmoon} + \\ & \cos i_{\leftmoon} \sin(\omega_{\leftmoon} + f_{\leftmoon}) \sin\Omega_{\leftmoon}).\end{aligned} \tag{43}$$

In this case the integration is done by expressing the mean anomaly in terms of the true anomaly of the third body: $dM_{\leftmoon} = (1 - e_{\leftmoon})^{3/2}/(e_{\leftmoon} \cos f_{\leftmoon} + 1)^2$. At this point the integration is performed,

yielding to:

$$\begin{aligned}\bar{\bar{\mathcal{R}}}_{\mathbb{C},2} =& \frac{\mu_{\mathbb{C}}}{32\, a_{\mathbb{C}}^3\,(1-e_{\mathbb{C}}^2\,)^{3/2}}\Big(30\, e^2 \cos\,2\omega \cos^2\Delta\Omega + \\ &+ (2+3\,e^2)(-5+3\cos 2\Delta\Omega) + \\ &6(2+3\,e^2+5e^2\cos 2\omega)\sin^2\Delta\Omega\cos^2 i_{\mathbb{C}} + \\ &- 6(-2-3\,e^2+5e^2\cos 2\omega)\cos^2 i(\sin^2\Delta\Omega+\cos^2\Delta\Omega\cos^2 i_{\mathbb{C}}\,) + \\ &- 60\, e^2 \sin 2\omega \sin\Delta\Omega\cos i_{\mathbb{C}}\,\sin i \sin i_{\mathbb{C}} + \\ &+ 6(2+3\,e^2-5\,e^2\cos 2\omega)\sin^2 i \sin^2 i_{\mathbb{C}} + \\ &+ 6\cos i(-5\,e^2\sin 2\omega\sin 2\Delta\Omega(1-\cos^2 i_{\mathbb{C}}\,) + \\ &+ 2(2+3\,e^2-5\,e^2\cos 2\omega)\cos\Delta\Omega\cos i_{\mathbb{C}}\,\sin i\cos i_{\mathbb{C}}\,)\Big),\end{aligned} \tag{44}$$

$$\begin{aligned}\bar{\bar{\mathcal{R}}}_{\mathbb{C},3} =& \frac{\mu_{\mathbb{C}}\,15a^3\,e\,e_{\mathbb{C}}}{512 a_{\mathbb{C}}^4\,(1-e_{\mathbb{C}}^2\,)^{5/2}}\Big(\cos\omega\cos\omega_{\mathbb{C}}\,\cos(\Omega-\Omega_{\mathbb{C}}\,) \\ &(35e^2\cos(2(\Omega_{\mathbb{C}}\,-\omega-\Omega)) + 35e^2\cos(2(\Omega_{\mathbb{C}}\,+\omega-\Omega)) + \\ &...\text{long expression}...\Big),\end{aligned} \tag{45}$$

$$\begin{aligned}\bar{\bar{\mathcal{R}}}_{\mathbb{C},4} =& \frac{3a^4\left(15e^4+40e^2+8\right)\left(3e_{\mathbb{C}}^2\,+2\right)\mu_{\mathbb{C}}}{128 a_{\mathbb{C}}^5\,\left(1-e_{\mathbb{C}}^2\,\right)^{7/2}} + \\ &\frac{9a^4\left(e_{\mathbb{C}}^2\,+2\right)\mu_{\mathbb{C}}}{1024 a_{\mathbb{C}}^5\,\left(1-e_{\mathbb{C}}^2\,\right)^{7/2}}\Big(35(e^2-1)^2(\cos i\cos\omega(\cos \mathrm{i}_{\mathbb{C}}\,\cos\omega_{\mathbb{C}} \\ &+ ...\text{long expression}...\Big).\end{aligned} \tag{46}$$

Note that, with respect to the analysis done in previous works,[8] here the eccentricity of the Moon's orbit about the Earth is retained. Indeed, in this case, the odd term is not null since the eccentricity of the third body is considered different from zero. The overall expression is function of:

$$\bar{\bar{\mathcal{R}}}_{\mathbb{C}}\, = \bar{\bar{\mathcal{R}}}_{\mathbb{C}}\,(a,\, e,\, i,\, \omega,\, \Omega-\Omega_{\mathbb{C}}\,,\, -,\, a_{\mathbb{C}}\,,\, e_{\mathbb{C}}\,,\, i_{\mathbb{C}}\,,\, \omega_{\mathbb{C}}\,;\, \mu_{\mathbb{C}}\,), \tag{47}$$

where the satellite semi-major axis a is a constant of motion.

Venus-Sun system Hamiltonian expression In this system, only the perturbations due to the Sun and J_2 are considered, since no natural satellites are present. The final double-averaged Hamiltonian expression is:

$$\bar{\bar{\mathcal{H}}} = \bar{\bar{\mathcal{H}}}(a,\, e,\, i,\, \omega,\, \Omega,\, -;\, \epsilon,\, r_{\odot},\, J_2,\, \mu,\, \mu_{\odot}). \tag{48}$$

Earth-Moon-Sun system Hamiltonian expression From the previous procedure, considering the effect of J_2, Sun and Moon disturbances, the final double-averaged Hamiltonian expression for the time evolution of the satellite's orbit is:

$$\bar{\bar{\mathcal{H}}} = \bar{\bar{\mathcal{H}}}(a,\, e,\, i,\, \omega,\, \Omega-\Omega_{\mathbb{C}}\,,\, -,\, a_{\mathbb{C}}\,,\, e_{\mathbb{C}}\,,\, i_{\mathbb{C}}\,,\, \omega_{\mathbb{C}}\,;\, \epsilon,\, r_{\odot},\, J_2,\, \mu,\, \mu_{\odot},\, \mu_{\mathbb{C}}\,). \tag{49}$$

Model Validation

First, the correct level of approximation is measured by comparing the single and the double-averaged model. Figure 1 shows the orbital propagation in time of a Earth' orbiter with certain initial conditions: it can be seen that the accuracy for the double-averaged model is very good in describing the long term evolution of the satellite. The reference Earth's orbit under study is an INTEGRAL-like orbit with the following initial conditions is considered (ephemeris taken at 22/03/2013*). Also a zoomed part is presented to see how the averaging procedure cancel out the short periodic oscillations in orbital elements.

Table 1. Orbital parameters of a INTEGRAL-like orbit.

a (km)	e (-)	i (deg)	ω (rad)	Ω (rad)	M (rad)
87705.22	0.8766	61.53	4.6385	2.2516	4.15

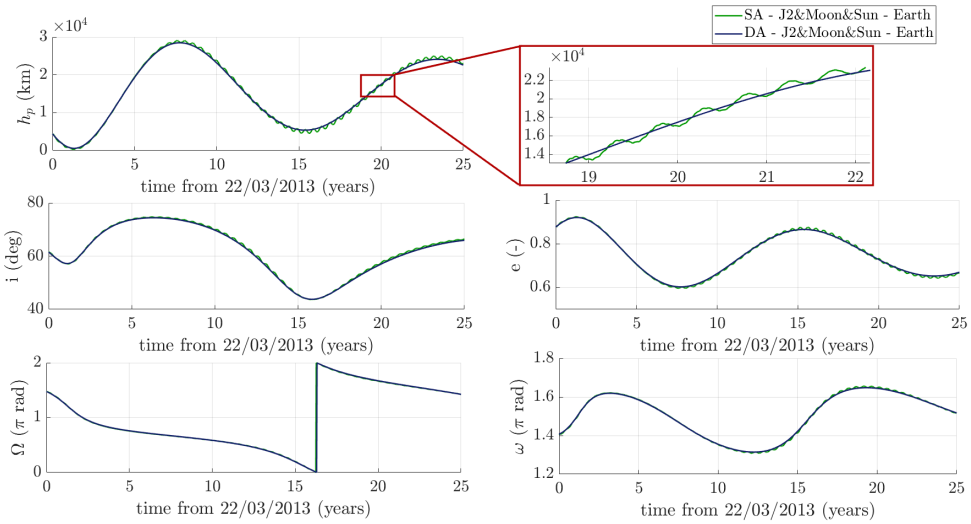

Figure 1. INTEGRAL satellite: comparison between the time evolution of the exact, single and double-averaged approximations (where SA is single-averaged and DA is double-averaged).

REDUCED HAMILTONIAN FORMULATION

After the double average, the Hamiltonian is non-autonomous two degrees of freedom system, with the time-dependencies stemming from the third bodies' ephemeris. To obtain a two-dimensional phase space representation it is necessary to reduce the number of variables of the problem: a one-degree-of-freedom Hamiltonian is necessary. Therefore, the aim of this section is to identify a technique to reduce the Hamiltonian formulation to a one-degree-of-freedom expression. The proposed double averaged model contains the influence of the satellite RAAN. For a satellite under the influence of J_2, Sun and Moon, the argument of the node appear in two different ways. In the Moon potential $\bar{\bar{\mathcal{R}}}_{\leftmoon}$ it appears as a combination of $\Omega - \Omega_{\leftmoon}$, while in the Sun effect $\bar{\bar{\mathcal{R}}}_{\odot}$, it is not coupled with the Sun node. The approach used to further reduce the system is based on a further averaging procedure, this time over the node of the satellite. This procedure is known as the *elimination of the node*.

*NASA JPL Horizon Web Interface: `https://ssd.jpl.nasa.gov/horizons.cgi`, latest visit on 10/2018

Node Elimination procedure

This approach is similar to represent the Hamiltonian function in a new frame, where the dependence on the RAAN is not present anymore. Nevertheless, the accuracy of this approximation shall be evaluated, to see whether it can correctly represent the orbital propagation. Starting from the double averaged Hamiltonian expressions for both Venus and Earth system, respectively in Eq. (48) and (49), the elimination of the node is performed with an integration over Ω:

$$\mathcal{H} = \frac{1}{2\pi} \int_0^{2\pi} \bar{\bar{\mathcal{H}}}\, d\Omega. \tag{50}$$

Performing this integration, the Hamiltonian expressions becomes:

Venus-Sun system:

$$\mathcal{H} = \mathcal{H}(a,\, e,\, i,\, \omega,\, -,\, -;\, \epsilon,\, r_\odot,\, J_2,\, \mu,\, \mu_\odot). \tag{51}$$

Earth-Moon-Sun system

$$\mathcal{H} = \mathcal{H}(a,\, e,\, i,\, \omega,\, -,\, -,\, a_\leftmoon\, ,\, e_\leftmoon\, ,\, i_\leftmoon\, ,\, \omega_\leftmoon\, ;\, \epsilon,\, r_\odot,\, J_2,\, \mu,\, \mu_\odot,\, \mu_\leftmoon\,). \tag{52}$$

In particular, by considering the orbital elements of the Moon and of the Sun constant in time, it becomes function of the satellite's Keplerian elements only, with a a constant of motion:

$$\mathcal{H} = \mathcal{H}(a,\, e,\, i,\, \omega,\, -,\, -;\, a_\leftmoon\, ,\, e_\leftmoon\, ,\, i_\leftmoon\, ,\, \omega_\leftmoon\ \epsilon,\, r_\odot,\, J_2,\, \mu,\, \mu_\odot,\, \mu_\leftmoon\,). \tag{53}$$

After the integration, a triple averaged model is produced: it does not depend anymore on the satellite node. Under the previous assumptions, the Hamiltonian formulation is a time-independent expression: hence, the Kozai parameter can be applied. It is a constant of motion in case the Hamiltonian is a time-invariant relation, as it is in Eq. (53), and it is defined as a function of the eccentricity and inclination:[12]

$$\Theta_{kozai} = (1 - e^2)\cos^2 i \tag{54}$$

This parameter is introduced to relate the inclination and the eccentricity variation in time. Since Θ_{kozai} is constant during the time evolution, the inclination can be written as a function of the eccentricity:

$$i = \arccos\Big(\frac{\Theta_{kozai,0}}{\sqrt{1-e^2}}\Big), \tag{55}$$

where $\Theta_{kozai,0}$ is related to the initial condition for orbit propagation at time t_0. And this results in a two degree of freedom Hamiltonian, since the semi-major axis is a constant of motion for the secular evolution of the satellite orbit: $a = a_0$.

$$\mathcal{H} = \mathcal{H}(-,\, e,\, -,\, \omega,\, -,\, -;\, a_0,\, e_0,\, i_0,\, a_\leftmoon\, ,\, e_\leftmoon\, ,\, i_\leftmoon\, ,\, \omega_\leftmoon\ \epsilon,\, r_\odot,\, J_2,\, \mu,\, \mu_\odot,\, \mu_\leftmoon\,). \tag{56}$$

Phase-Space Maps

The new simplified Hamiltonian dynamically depends on two variables: eccentricity and perigee anomaly (e, ω). To produce the two-dimensional maps, each phase space is produced in terms of fixed semi-major axis, which corresponds to the initial condition for the orbit propagation. This

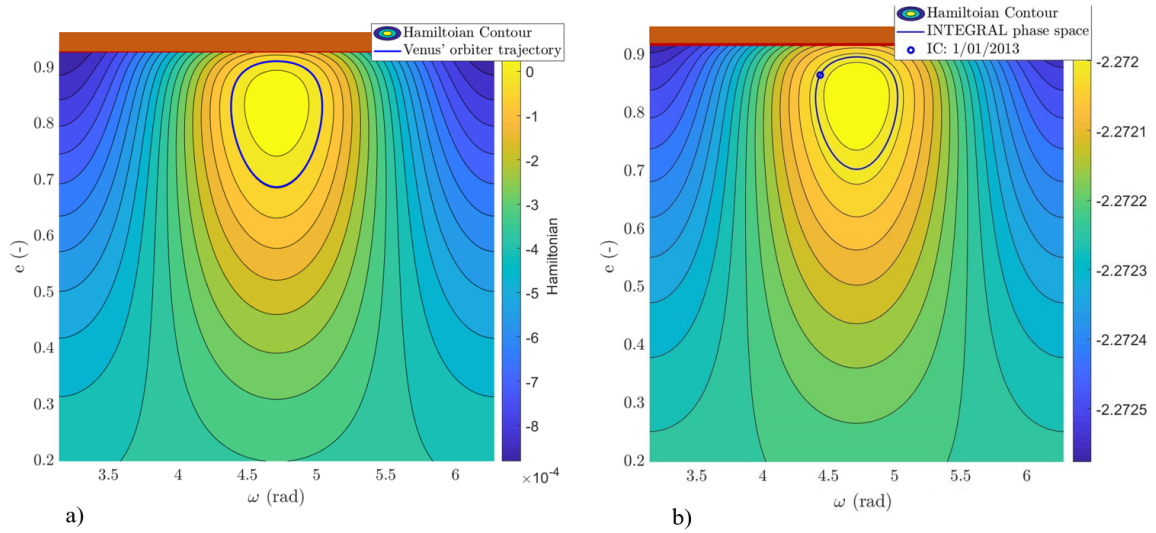

Figure 2. a) Venus' phase space with $a_0 = 87000$ km, $e_0 = 0.87$, $i_0 = 60°$. The blue trajectory represents the orbit evolution in time of the Venus' orbiter. b) INTEGRAL phase space with $a_0 = 87839$ km, $e_0 = 0.87$, $i_0 = 61.5°$. The blue trajectory represents the orbit evolution in time of the INTEGRAL satellite.

means that each phase space is related to a defined value of a_0, and therefore to a fixed orbital initial condition. To produce the two-dimensional maps, a reference condition is chosen in terms of (e_0, ω_0), for the computation of the Kozai parameter at time t_0: $\Theta_{kozai,0}$. The phase space maps are produced by computing the contour plot of the Hamiltonian function. From a generic initial condition, the Hamiltonian expresses the time evolution of eccentricity and perigee anomaly of the satellite orbit. The Hamiltonian function is therefore defined for a specific initial condition $(e_0,\ \omega_0)$:

$$\mathcal{F} = \mathcal{H}(e, \omega) - \mathcal{H}_0(e_0, \omega_0), \tag{57}$$

where (e_0, ω_0) are the initial condition for the orbital parameters. The phase space maps are now presented for the two cases of study in Figure 2. First, a Venus orbiter is analyzed under the Sun third body effect, then an INTEGRAL-like satellite is considered in the Earth-Moon-Sun system.

END-OF-LIFE MANOEUVRE DESIGN

The strategy developed in this work consists of targeting a specific condition for the disposal in terms of Keplerian parameters. A single maneuver is performed during the natural evolution of the spacecraft. The aim of the maneuver is to produce a change in the orbital parameter so that the resulting trajectory evolution in time produces a variation in time evolution to reach the disposal condition.[3] From the target perigee to assess the atmospheric re-entry, it is possible to get the corresponding critical eccentricity value e_{cr} that the orbit should have to verify the condition:

$$e_{cr} = 1 - \frac{h_{p,min} + R_\alpha}{a} \tag{58}$$

In particular, the maneuver designed in this work is the atmospheric re-entry at the end-of-life by applying a single impulsive maneuver Δv. The phase space representation is very intuitive and allows the visualization of the maneuver effect. The delta-v will change the condition of the orbital

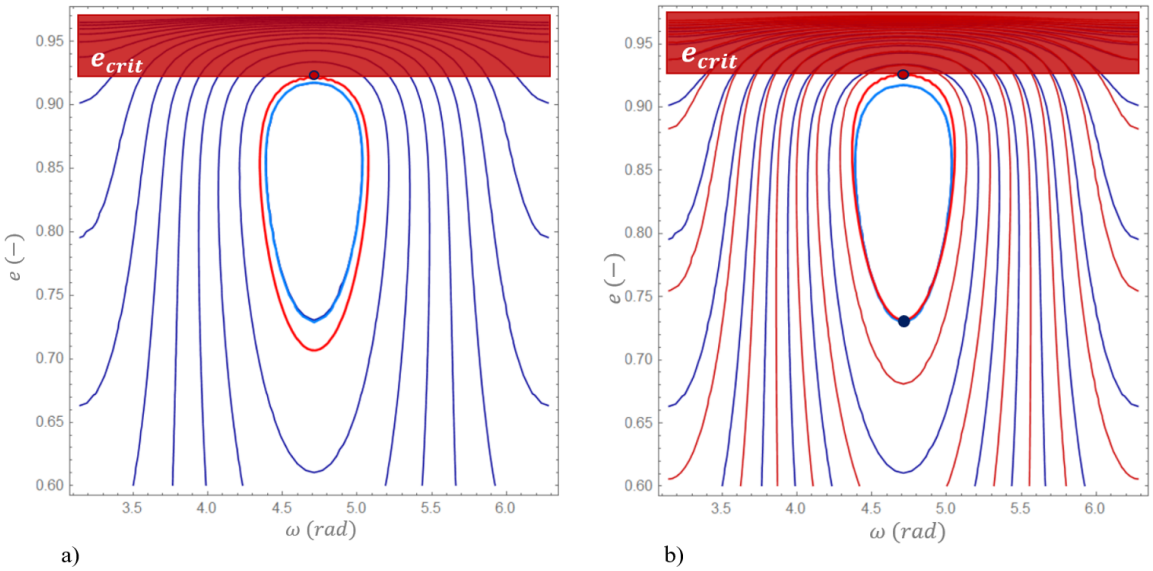

Figure 3. a) Manoeuvre in the same phase space ($a_0 = 87000$ km). The light blue trajectory is the evolution from the initial condition, the red one is the evolution of the orbital condition after the maneuver. b) Maneuver among two phase space (form the blue one to the red one). The light blue trajectory is the evolution from the initial condition, the red one is the evolution of the orbital condition after the maneuver.

parameter so that the final trajectory in the phase space would target the critical eccentricity. This means that the final trajectory is tangent to that value, indicating that in time the re-entry condition is achieved.

A first simple approach is to target another trajectory in the same phase space, as in Figure 3a, for which the maximum eccentricity is the critical one. The impulsive maneuver shall provide a variation in eccentricity and anomaly of perigee only, maintaining the semi-major axis an invariant. A second approach is to provide an impulsive maneuver, which changes also the semi-major axis. This results in a variation of the phase space representation, as in Figure 3b. Depending on the new value of the semi-major axis, the Hamiltonian contour line could be translated up or down in the phase space. For a reduction of a, the phase space translates towards higher values of the eccentricity, enhancing the disposal condition. The computation of the maximum eccentricity condition could be done in two ways, explained in next subsections.

Semi-analytical method

After the application of the delta-v, the new Keplerian elements are propagated in time using the double-averaged model of Eq. (48) and (49). This procedure is efficient but requires some computational time: for each new condition after the delta-v, a time propagation is required to check for the maximum eccentricity value, this approached was followed in several analyses in literature.[3,8]

Fully-analytical method

This new procedure is implemented in this work starting from the triple-averaged model resulting from the node elimination procedure. From the Hamiltonian expression of the time evolution of

the satellite orbit, $\mathcal{F} = \mathcal{H}(e, \omega) - \mathcal{H}(e_0, \omega_0)$, the maximum eccentricity condition can be simply computed from the stationary points of the function:

$$e_{cr} = \max(\mathcal{F}(e, \omega)) \tag{59}$$

This procedure has several advantages: computing analytically the stationary point of a function ($\mathcal{F}$) is a much more computationally efficient method than the semi-analytical one. In addition, this means that $\mathcal{F}$ can be used to compute the orbital evolution of the satellite in time without any numerical integration for orbit propagation at all.

Venus' orbiter disposal design

The atmospheric entry for the disposal strategy of a Venus' orbiter was adopted in the past for some missions, such as the Venus Express, which ends its operative life with a de-orbit trajectory.[13] The de-orbit happens when the perigee altitude is below the atmospheric interface. For Venus express, the drag effect starts being significant below 200 km.* For this reason, the atmospheric entry condition was set at 130 km for Venus' orbiter:

$$h_{p,min} = \min\{h_{p,min}(t)\} < 130\,\mathrm{km} \tag{60}$$

The disposal was computed through an optimization procedure. This is necessary to evaluate which is the optimal impulse that provides the desired solution, not only the magnitude of the impulse is optimized, but also its direction. In particular, the optimization is implemented for different initial conditions in time from the natural evolution of the satellite orbit. This aims to determine the optimal parameters for the definition of the $\mathbf{\Delta v}$ impulse and the optimal true anomaly for the maneuver f_m. An optimal set of parameter is defined from literature:[3] $\mathbf{x} = [\alpha,\, \beta,\, \Delta v,\, f_m]$ and a multi-objective optimization[14] was imposed to minimize the difference between the maximum eccentricity of the new orbital evolution after the manoeuvre and the target condition. The parameters α and β represents the in and out of plane angle of the maneuver's direction Δv.

Numerical results for minimum and maximum eccentricity condition The first optimization was done for the maximum and the minimum eccentricity point to define the interval of the maneuver cost. The maneuver was modeled both with the fully-analytical and semi-analytical approach to verify the accuracy of the results. As reported in Table 2, the maneuver is more expensive if given when the time history of the orbit eccentricity reaches its maximum. In Figure 4a, the two manoeuvres are reported in the phase space. The manoeuvre at the maximum eccentricity (M2) is more expensive since it results in a direct reduction of the perigee altitude to the critical condition. On the other hand, for the minimum eccentricity (M1) condition, it results in a tangent manoeuvre: the consumption of propellant is less. M2 consists in a manoeuvre at the apogee to change the perigee altitude, increasing instantaneously the eccentricity of the orbit. On the other hand, the manoeuvre at M1 maintains constant the eccentricity of the orbit, resulting in a δe almost zero, the delta-v produces a variation in the semi-major axis, decreasing it and in a reduction of the orbital inclination. Moreover, by comparing the different levels of approximation of the secular evolution for Venus-Sun system, even for a very long time of propagation, the single, double and triple models provide the same results, as shown in Figure 4b. This validates the fully-analytical model for orbital maneuver computation in case of the Venus-Sun system.

*from NASA Venus Express Mission Information: `https://pds.nasa.gov/ds-view/pds/viewMissionProfile.jsp?MISSION_NAME=VENUS%20EXPRESS`, last accessed: 11/2018

Table 2. Results for maximum and minimum eccentricity condition of the Venus' orbiter.

	Semi-analytical propagation	Fully-analytical solution
Manoeuvre - M1		
Δv at e_{min}	60 m/s	57 m/s
Minimum perigee altitude	130 km	130 km
Computational time	1 h	3 min
Manoeuvre - M2		
Δv at e_{max}	84 m/s	86 m/s
Minimum perigee altitude	130 km	130 km
Computational time	1 h	5 min

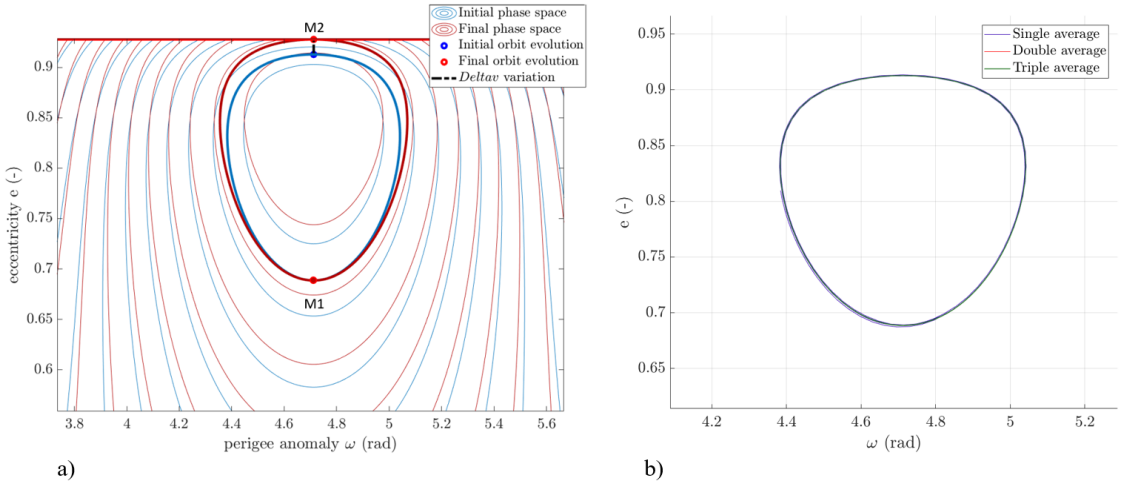

Figure 4. a) Phase space trajectory in (ω, e) to target the critical condition for the re-entry. The initial phase space is in blue line, while the final phase space is in red. b) Comparison of single, double and triple-averaged model to describe the Venus' orbiter secular evolution. The three models are completely equivalent.

INTEGRAL disposal design

The end-of-life strategy of the INTEGRAL mission was already studied in many works.[3,15] In both works, they exploit a semi-analytical orbit propagator to describe with high fidelity the orbit motion of the satellite. The typical target perigee altitude for an earth re-entry is equal or lower than 80 km.[3] Moreover since this condition refers to missions with a lower initial perigee than INTEGRAL, it is assumed a perigee equal or below 50 km. This is due to the higher velocity at the atmospheric interface, which could results in a partial fragmentation or the bouncing on the atmosphere if the target perigee is above 50 km.

Numerical results for minimum and maximum eccentricity condition The first optimization was set to define the cost of the maneuver at the minimum and at the maximum eccentricity condition. Two maneuvers were investigated: M_1 at the minimum eccentricity condition, and M_2 at the maximum eccentricity condition. The maneuver was modeled both with the semi-analytical propagation optimization and with the fully-analytical approach in the phase space. The results are shown in Table 3.

Table 3. Results for maximum and minimum eccentricity condition of the INTEGRAL satellite.

	Semi-analytical propagation	Fully-analytical solution
Manoeuvre - M1		
Δv at e_{min}	45.7 m/s	106 m/s
Minimum perigee altitude	50.0 km	50.0 km
Computational time	3 h	3 min
Manoeuvre - M2		
Δv at e_{max}	97 m/s	67 m/s
Minimum perigee altitude	50.0 km	50.0 km
Computational time	3 h	5 min

The results from the fully-analytical model are comparable with the results in a previous study.[4] The Figure 5a shows how the phase space change after the manoeuvre. Both for the minimum and the maximum eccentricity condition, the spacecraft reaches the same final trajectory. Nevertheless, the results from the fully-analytical method are just the opposite than the results from the semi-analytical one, and can be used only for very preliminary estimation of the delta-v magnitude. This difference is the consequence of the non-accuracy of the triple averaged model used to recover the maximum eccentricity, see the comparison of the model in Figure 5b. In fact, the semi-analytical model results are in accordance with the numerical disposal options obtained in literature analysis for the INTEGRAL disposal condition.[3] For this reason, the triple averaged model can be used just for a very preliminary estimation of the order of magnitude of the manoeuvre effort.

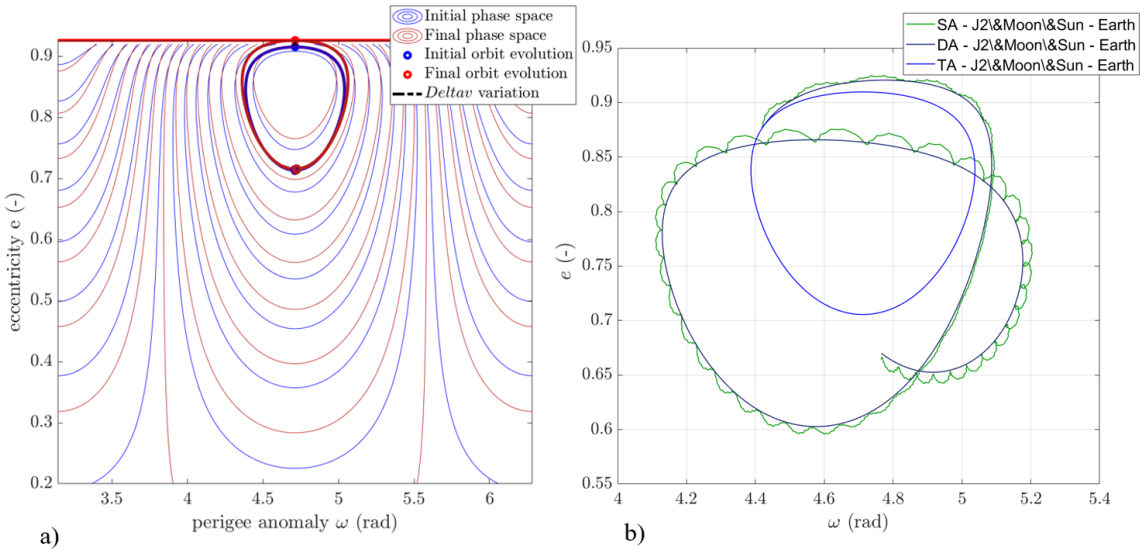

Figure 5. a) INTEGRAL phase space trajectory in (ω, e) to target the critical condition for the re-entry. The initial phase space is in blue line, while the final phase space is in red. b) Comparison of single, double and triple-averaged models to describe the INTEGRAL secular evolution. The triple averaged-model can be used just for a very preliminary estimation.

Problem of the Node Elimination for the Earth-Moon-Sun case

The results, given by the Earth-Moon-Sun model, highlight the limitations of the triple-averaged model in some cases. In particular, the model developed correctly works for a system where the relative inclination of the perturber upon the equator is negligible. As a result, approximating the Sun and the Moon on the equatorial plane provides good results as well as the Venus' case. Nevertheless, the results for the equatorial case reveal how the Earth-Moon-Sun system has a complex behavior. It is not as simple as the Venus' one, for which the Lidov-Kozai approximation correctly works, as in Figure 4b. This suggests that different approaches for the elimination of the node should be used. In fact, the idea is very promising since allows the determination of the critical eccentricity (maximum eccentricity value in time) without propagating the dynamics, but simply by solving the Hamiltonian equation. The limitation of the present model is that the elimination of the satellite's node is not a trivial process in the case of perturbers in different orbital planes. This is a very complex problem and should be addressed in future works and requires that the dynamics are regular and the phase-space can accurately be described by an 1-DOF model.

The low accuracy is therefore caused by the elimination of the dependence in the Hamiltonian expression from the $\Omega - \Omega_{\leftmoon}$, and the other assumptions done to reduced the formulation to a one degree-of-freedom problem. In fact, the Moon node has a non-linear variation on the equatorial frame and its coupling effect with the satellite node causes complex dynamical behavior of the secular evolution of the satellite orbit. Moreover, both the inclination and the argument of perigee of the Moon are considered constant, when they actually vary in time. Therefore, the reduction procedure drops some important contribution for the determination of the secular and long-term satellite evolution.

CONCLUSIONS

The proposed analytical model based on the reduced Hamiltonian formulation is able to describe exactly the dynamical evolution of a satellite under the coupling effect of the planet's oblateness and the third body attraction only for some peculiar cases. In particular, if the third body effect does not introduce significant dynamical coupling between the orbital plane of the satellite and the third body, the analytical model can compute the orbital evolution exploiting just one single equation. This can be used to surf among the phase space to find the optimal maneuver to reach the target condition, as the disposal atmospheric re-entry for a Venus' orbiter. In fact, the Venus-Sun system is a proper system to apply the model, since the satellite moves in the phase space under the coupling effect of the Sun and J_2. Moreover, the obliquity of the ecliptic for Venus is small enough to consider as a first approximation that the equator and the ecliptic lie on the same plane.

The computation of the optimal maneuver for an atmospheric re-entry using the fully-analytical approach is computational more efficient than the semi-analytical method, which involves the integration of the orbital element propagation in time. In particular, the computational time reduces from more than 1 hours in the semi-analytical case to about 3-5 minutes in the fully-analytical one. The main drawback of this model appears in the Earth-Moon-Sun system. This system is very complex, and the Hamiltonian reduction is based on too stringent hypotheses to describe in an accurate way the real satellite dynamics. The problematic arises from the node elimination. Since the right ascension of the satellite is coupled with the Moon node, by eliminating Ω, very complex dynamics are discharged. The fully-analytical model is not accurate for the Earth's system, and therefore can only be used for a very preliminary analysis of the order of magnitude of the maneuver effort.

On the other hand, the semi-analytical model, considering the orbit propagation in time produces suitable results for the disposal strategy of the INTEGRAL mission.

This work opens to a variety of future developments. First, the node reduction works perfectly for a low inclined perturbing body, which orbit can be approximated to be on the equator. On the other hand, for the Earth-Sun-Moon system, this opens to different approaches. Since the main achievement is the optimal single maneuver design for the Venus-Sun system, future works could investigate more accurate analysis comparing the triple-averaged model and the second-averaged model with a full numerical propagation of the orbit evolution for a future mission. Moreover, the phase space maps of the triple-averaged Hamiltonian could be used also for other applications, like frozen conditions for a Venus' orbiter. On the other hand, for the Earth-Moon-Sun system, the nodal reduction should be analyzed. A first study could investigate the feasibility of finding a solution to the 2.5 degrees of freedom Hamiltonian, that is produced after the double averaging. Some works were already implemented in this direction.[1] Moreover, the need to reduce the computational time is related to the possibility of generating software that can compute the optimal disposal trajectory from the current ephemeris of the satellite. This is fundamental during the design of the mission since it allows the correct dimension of each satellite's subsystem. This idea is very revolutionary and could be achieved only by solving the satellite dynamics in a fully-analytical way, as it was done in this work.

ACKNOWLEDGMENT

This project has received funding from the European Research Council (ERC) under the European Unions Horizon 2020 research and innovation program (grant agreement No 679086 - COMPASS).

REFERENCES

[1] I. Gkolias, M. Lara, and C. Colombo, "An Ecliptic Perspective for Analytical Satellite Theories," *AAS/AIAA Astrodynamics Specialist Conference. San Diego, California, U.S.A.*, 19-23 August 2018, pp. 1–15.

[2] T. Sweetser, "How to Maneuver Around in Eccentricity Vector Space," *AIAA/AAS Astrodynamics Specialist Conference. Toronto, Ontario, Canada*, 2-5 August 2010, p. 7523.

[3] C. Colombo, F. Letizia, E. M. Alessi, M. Landgraf, *et al.*, "End-of-life Earth re-entry for highly elliptical orbits: the INTEGRAL mission," *The 24th AAS/AIAA space flight mechanics meeting. Santa Fe, New Mexico, U.S.A.*, 26-30 January 2014, pp. 26–30.

[4] C. Colombo, E. M. Alessi, and M. Landgraf, "End-of-life Disposal of spacecraft in Highly elliptical Orbits by Means of Luni-Solar Perturbations and Moon Resonances," *6th European Conference on Space Debris. Darmstadt, Germany.*, Vol. 723, 22 - 25 April 2013.

[5] C. Colombo, E. M. Alessi, W. v. d. Weg, S. Soldini, F. Letizia, M. Vetrisano, M. Vasile, A. Rossi, and M. Landgraf, "End-of-life disposal concepts for Libration Point Orbit and Highly Elliptical Orbit missions," *Acta Astronautica*, Vol. 110, 2015, pp. 298–312.

[6] D. A. Vallado, *Fundamentals of astrodynamics and applications*, Vol. 12. Springer Science & Business Media, 2001.

[7] B. Kaufman, "Variation of parameters and the long-term behavior of planetary orbiters," *Astrodynamics Conference. Santa Barbara, California, U.S.A.*, 19-21 August 1970, p. 1055.

[8] C. Colombo, "Long-term evolution of highly-elliptical orbits: luni-solar perturbation effects for stability and re-entry," *25th AAS/AIAA Space Flight Mechanics Meeting. Williamsburg, Virginia, U.S.A.*, 11-15 January 2015.

[9] C.-C. G. Chao, *Applied orbit perturbation and maintenance*. American Institute of Aeronautics and Astronautics, Inc., 2005.

[10] A. J. Rosengren, E. M. Alessi, A. Rossi, and G. B. Valsecchi, "Chaos in navigation satellite orbits caused by the perturbed motion of the Moon," *Monthly Notices of the Royal Astronomical Society*, Vol. 449, No. 4, 2015, pp. 3522–3526.

[11] S. Breiter, "Lunisolar resonances revisited," *Celestial Mechanics and Dynamical Astronomy*, Vol. 81, No. 1-2, 2001, pp. 81–91.

[12] Y. Kozai, "Secular perturbations of asteroids with high inclination and eccentricity," *The Astronomical Journal*, Vol. 67, 1962, p. 591.

[13] H. Svedhem, D. Titov, F. Taylor, and O. Witasse, "Venus express mission," *Journal of Geophysical Research: Planets*, Vol. 114, No. E5, 2009.

[14] A. Shirazi, "Multi-objective optimization of orbit transfer trajectory using imperialist competitive algorithm," *Aerospace Conference, 2017 IEEE. Big Sky, Montana, U.S.A.*, IEEE, 2017, pp. 1–14.

[15] R. Armellin, J. F. San-Juan, and M. Lara, "End-of-life disposal of high elliptical orbit missions: The case of INTEGRAL," *Advances in Space Research*, Vol. 56, No. 3, 2015, pp. 479–493.